FIELD VALIDATION OF THE BACKWARD-IN-TIME ADVECTION DISPERSION THEORY

J.L. Wilson[1,] and J. Liu[2], [1]Department of Earth and Environmental Science, New Mexico Institute of Mining and Technology, Socorro, NM, 87801, Phone: 505-835-5308, FAX: 505-835-6436, and [2]Environmental Systems and Technology, Inc., Blacksburg, VA*

ABSTRACT We have recently developed a theory that can be used to locate the source of contamination captured by a pumping well [1]. Accounting for advection, dispersion, linear-equilibrium sorption, aquifer heterogeneity, and regional natural recharge, the theory is based on the concept of travel time probability. This probability describes the time for a particle to travel from a source location to the pumping well, and can be directly computed by solving adjoint partial differential equations backwards-in-time, with a third type probability boundary condition at the pumping well. We apply a two-dimensional version of the theory, implemented numerically using the Laplace Transform Galerkin method, to the analysis of a recent tracer test conducted at the Borden Site in Ontario, Canada [2]. The test was designed to validate common conceptual models of pumping well capture zones. Tracers were injected at 15 locations upgradient of a pumping well. Their arrival in the well was observed with weekly concentration measurements. A single two-dimensional backward-in-time simulation was used to predict separate travel time probabilities for each injection site. These were compared to normalized experimental breakthrough curves, and arriving tracer mass was assigned to 11 of the injection locations. Tracer from 4 injection sites was predicted to miss the pumping well. The assignments of mass and source location and the predicted tracer recovery compare favorably with independent interpretations of the experiment which were based on multiple three-dimensional forward simulations [3]. Satisfactory performance of the method on the field test data supports its validation as a standard tool and certainly demonstrates its practical use.

KEYWORDS: ground water, modeling, contamination, characterization

INTRODUCTION

When pollution is observed in a monitoring or pumping well it is often not known where the pollution comes from. This is a particularly important issue when designing or operating monitoring or remediation systems, assigning liability or responsibility, or assessing risk. A new mathematical modeling algorithm was introduced by Wilson and Liu [1, 4, 5] to address this and related issues involving monitoring, remediation, and water supply well head protection. By solving adjoint stochastic differential equations backwards-in-time, the method provides time- or space-dependent probability maps for the origin of water found in a well [6]. Using one-dimensional continuum models, Wilson and Liu [1] successfully tested the hypothesis that backward problems can be formulated and solved that account for advection, dispersion, first order decay, linear equilibrium adsorption, and non-equilibrium adsorption.

By proper selection of boundary conditions at the well, one of two types of probability map is obtained with one backwards-in-time run of a transport computer model. The first type of map is called a travel time probability map. It describes how long it

*To whom all correspondence should be addressed (email: jwilson@nmt.edu).

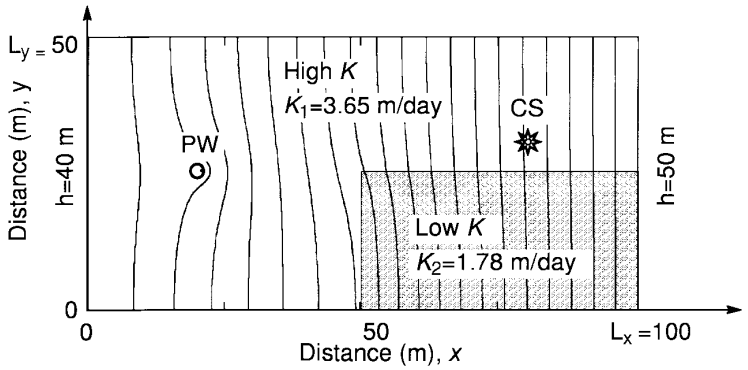

FIGURE 1. EXAMPLE PROBLEM DOMAIN. A PUMPING WELL (PW) IS LOCATED AT (20, 25), AND THE DISSOLVED CONTAMINATION SOURCE (CS) IS LOCATED AT (80, 30). HYDRAULIC HEADS ARE CONTOURED WITH AN INTERVAL OF 0.5 M.

takes water to move from some prescribed location in the aquifer to the well. It can be used to describe a well-head protection area or be convoluted with estimated pollutant spatial concentrations to predict arriving pollutant concentrations. In the backward problem third type boundary conditions are used at the pumping well when calculating travel time probabilities. The second type of map defines the origin of water observed or produced in the well. It gives the probability that pollution originating at some location in the aquifer will arrive at the well some specific time *t* later. Called a location probability map, it is useful in identifying possible sources of past pollution and for monitoring design. Earlier versions of location maps have been produced by a backward-in-time random walk approach [7-11]

Insomuch as it appears that the backwards method works in theory, we decided to investigate its practical application, including a validation and demonstration, using the results of a field test. In this paper we first implement and describe the method on a few simple idealized two-dimensional problems using a standard numerical simulation code of flow and transport. We then apply the method using data collected at a recent field tracer study of capture zones. Satisfactory performance of the method on the field test data supports its possible validation as a standard tool and certainly demonstrates its practical use. Because of the nature of the field test, only travel time probabilities can be studied. We do not consider location probabilities in this paper.

BACKWARD-IN-TIME MODEL FOR A TWO-DIMENSIONAL AQUIFER

We develop and illustrate the two-dimensional version of the approach using the hypothetical aquifer shown in Figure 1. The 100 m x 50 m rectangular aquifer is heterogeneous, consisting of two sub-domains: high hydraulic conductivity and low hydraulic conductivity. The ground water flows from right to left. We create backward-in-time travel time and location probability maps for the downstream pumping well located toward the left-hand side. Before that we will illustrate the traditional forward-in-time approach by injecting contamination at the upstream source, labeled CS, located on the right side of the figure, and watch it move downstream

and into the well. Preliminary results have been previously presented [5].

The forward-in-time (FIT) contaminant transport and backward-in-time (BIT) probability models are numerically simulated using the Laplace transform-in-time Galerkin finite element method [12]. The computer code, FRACTRAN, written by Sudicky and McLaren [13], was modified to account for natural recharge and non-equilibrium sorption and to implement the appropriate BIT third type boundary conditions at sinks and source.

Contaminant transport in a two-dimensional heterogeneous aquifer

The steady flow field in Figure 1 is described by the field equation:

$$\frac{\partial}{\partial x_i}\left(KB\frac{\partial h}{\partial x_j}\right) - \delta\left(X - X_1\right)Q_o = 0, \tag{1}$$

where x_i, $i = 1, 2$ are the x, y coordinates of the domain, $X = (x, y)$; h is hydraulic head [L]; K is the isotropic but non-homogeneous hydraulic conductivity [L/T]; B is the aquifer thickness; and Q_o is the pumping rate [L^3/T] at $X_1 = (x_1, y_1)$. For the example problem, constant head boundaries are prescribed on the left and right, with no flow boundaries at the top and bottom:

$$h = h_1, \; at \; x = 0; \; h = h_2, \; at \; x = L_x \tag{2a}$$

$$\frac{\partial h}{\partial y} = 0, \; at \; y = 0; \; y = L_y, \tag{2b}$$

where L_x and L_y are the length and width of the domain. The parameters for the example problem are summarized in Table 1, and the simulated heads are contoured in Figure 1. The ground water flow direction is normal to the contour of the hydraulic head.

To illustrate the FIT approach, a contaminant is introduced at location CS, $X_o = (x_o, y_o)$, at time $t = 0$. In the aquifer, the aqueous phase resident concentration $C^r(X, t)$ for a non-reactive contaminant is described by:

$$\frac{\partial C^r}{\partial t} = \frac{\partial}{\partial x_i}\left(D_{ij}\frac{\partial C^r}{\partial x_j}\right) - V_i\frac{\partial C^r}{\partial x_i}, \tag{3}$$

where $C^r = C^r(X, t)$ is the resident concentration, $V_i(X) = -(K/\theta)\partial h/\partial x_i$ is the velocity vector computed from the flow solution, θ is the porosity, and D_{ij} $(i, j = 1, 2)$ is the second-order dispersion tensor. For the example in Figure 1, the boundary and initial conditions for the mass transport are expressed as:

$$\frac{\partial C^r}{\partial x} = 0, \; at \; x = 0; \; C^r = 0, \; at \; x = L_x \tag{4a}$$

$$\frac{\partial C^r}{\partial y} = 0, \; at \; y = 0; \; \frac{\partial C^r}{\partial y} = 0, \; at \; y = L_y \tag{4b}$$

$$\lim_{r\to 0}\int_S \frac{\partial C^r}{\partial r}dS = 0, \; at \; \; pumping \; \; well \; \left(x_1, y_1\right) \tag{4c}$$

$$C^r = \frac{M}{\theta B}\delta\left(X - X_O\right), \; \; for \; \; t = 0, \tag{4d}$$

where M is the released contaminant mass of 0.356 grams at $X_o = (x_o, y_o)$, S is the boundary around the pumping well at radius, r. For the pumping well, the dispersive solute flux is equal to zero. The initial condition is a Dirac function at point (x_o, y_o), where $\delta(X\text{-}X_o) = \delta(x\text{-}x_o, y\text{-}y_o)$. The parameters for contaminant transport are listed in Table 1.

Given a particular source location, this forward-in-time (FIT) model can be solved for resident concentration as a function of time and space. The FIT simulation for the source CS at (80, 30) is shown in Figure 2 for three times after injection: t = 30 days, 40 days, and 60 days. The injected contamination plume moves downstream, spreads, dilutes, and finally is extracted by the pumping well. This figure shows the combined effects of advection, dispersion, and aquifer heterogeneity.

TABLE 1. PARAMETERS USED IN THE SIMULATIONS.

Parameter	Hypothetical example	Borden tracer test
Domain	100 m x 50 m	30 m x 30 m
Hydraulic conductivity $K_x = K_y$,	3.56 m/day in high K sub-domain 1.78 m/day in low K sub-domain	7.09 m/day[a]
Longitudinal dispersivity a_L	0.4 m	0.08 m[a]
Transverse dispersivity a_T	0.2 m	0.001 m[a]
Diffusion coef. D[a]	3.0E-4 m^2/day	3.0E-4 m^2/day
Porosity θ	0.35	0.33[a]
Aquifer thickness B	1.0 m	7.3 m[a]
Pumping well location (x_o, y_o)	(20m, 25m)	(15m, 20m)
Pumping rate Q_o	5.0 m^3/day	2.16 m^3/day[a]
Boundary conditions or gradient data for ground water flow	h_1 = 40 m at x = 0 m, h_2 = 50 m at x = 50 m $\partial h/\partial y$ = 0 on top and bottom boundaries	time (days) J_a β 0-66 .....0.0041, 25.4° 67-118 .....0.0038, 9.0° 118-124 .....0.0029, -3.5°
FIT Transport Model		
Boundary conditions	C^r = 0 at the right boundary, $\partial C^r/\partial x_i$ = 0; otherwise	$\partial C^r/\partial x_i$ = 0 all sides
Initial condition	$C^r = [M/(B\theta)]\ \delta(X-X_o)$ for t = 0	$C^r = [M/(B\theta)]\ \delta(X-X_o)$ for t = 0
BIT model		
Boundary conditions	3rd type BC at pumping well; $f_\tau = 0$ at $x = L_x$; $\partial f_\tau/\partial x_i = 0$ otherwise	3rd type BC at pumping well; $\partial f_\tau/\partial x_i = 0$ otherwise
Initial condition	$f_\tau = 0$ for $\tau = 0$	$f_\tau = 0$ for $\tau = 0$
Grid Characteristics		
element size elements nodes	$\Delta x = \Delta y$ = 0.5 m; 20,000 20,301	$\Delta x = \Delta y$ = 0.2 m; 22,500 22,801

[a]After Linderfelt [3].

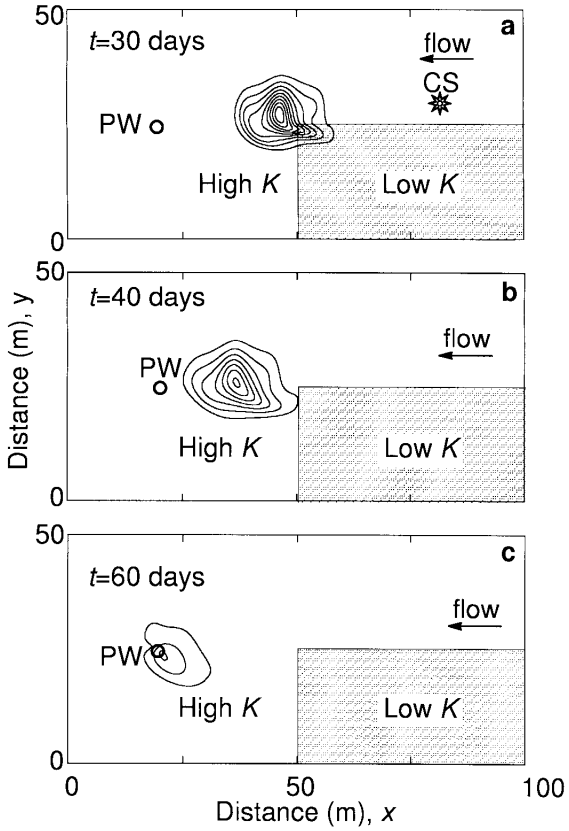

FIGURE 2. TWO-DIMENSIONAL TRANSPORT OF A CONTAMINANT PLUME IN A HETEROGENEOUS AQUIFER. FIGURES a-c SHOW THE PLUMES FOR 30 DAYS, 40 DAYS, AND 60 DAYS, RESPECTIVELY. THE OUTERMOST CONTOUR LINE REPRESENTS 0.004 (mg/l); THE CONTOUR INTERVAL IS 0.004 (mg/l).

The forward-in-time model for arrival time probability

We can apply Equations 3 and 4 to the problem of determining the contaminant flux-concentration arriving at the pumping well. The arriving aqueous phase flux concentration, $C^f(X, t)$, is equal to the resident concentration, $C^f(X, t) = C^r(X, t)$, because of the boundary condition in Equation 4c. The arrival time probability density function, $f_t(t \mid X_o)$ describes the probability that a non-reacting contaminant particle, released at location (x_o, y_o) at time, $t = 0$, will reach the pumping well at (x_1, y_1) in time t. The arrival time PDF is obtained from the normalized flux concentration:

$$f_t(t|X_O) = \frac{Q_O C^f(X_1,t)}{M}. \quad (5)$$

Here $f_t(t \mid X_o)$ is the arrival time PDF for a given source location, $X_o = (x_o, y_o)$, Q_o is the pumping rate at the pumping well, located at $X_1 = (x_1, y_1)$, and M is the total mass released at the source location. Example results from this type of FIT calculation for the arrival time PDF are given later, in Figure 4, for two different upstream injection points (Figure 4a shows the arrival time distribution for source CS).

It is clear that we can compute the arrival time PDF for a given source location, X_o, but what happens if we don't know where the source is located? Suppose that all we observe is the contamination concentration in the pumping well. Of course, it is possible to simulate the arrival time PDF numerically for each possible source location, but if there are a large number of these it would be very expensive in terms of time and computational resources. Worse, what if we do not know where the possible sources are?

The backward-in-time model for travel time probability

The travel time PDF can be directly computed using the new backward-in-time method. The two-dimensional travel time PDF, $f_\tau(\tau \mid X)$, for a travel time, τ, from some location $X = (x, y)$ to pumping well location (x_1, y_1), can be from an adjoint version of the standard advection-dispersion equation by replacing the concentration with $f_\tau(\tau \mid X)$, and replacing V in the forward problem by $-V$ (and t with $-\tau$):

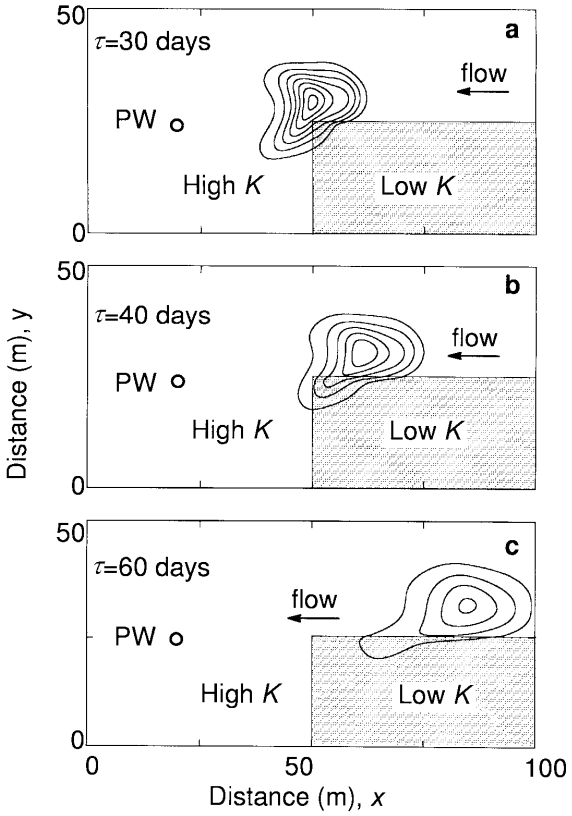

FIGURE 3. TWO-DIMENSIONAL TRAVEL TIME PDF FOR THE WELL IN THE HETEROGENEOUS AQUIFER. THE OUTERMOST CONTOUR LINE REPRESENTS A PROBABILITY LEVEL OF 0.02, AND THE CONTOUR INTERVAL IS 0.02, IN UNITS OF 1 DAY^{-1}. FIGURES a-c SHOW THE TRAVEL TIME PDF FOR 30 DAYS, 40 DAYS, AND 60 DAYS, RESPECTIVELY.

$$\frac{\partial f_\tau}{\partial \tau} = \frac{\partial}{\partial x_i}\left(D_{ij}\frac{\partial f_\tau}{\partial x_j}\right) + V_i\frac{\partial f_\tau}{\partial x_i}, \tag{6}$$

where $f_\tau = f_\tau(\tau / X)$ is travel time PDF, and i, j = 1, 2. In this example, the adjoint boundary and initial conditions are as follows:

$$\frac{\partial f_\tau}{\partial x} = 0, \; at \; x = 0; \quad f_\tau = 0, \; at \; x = L_x \tag{7a}$$

$$\frac{\partial f_\tau}{\partial y} = 0, \; at \; y = 0; \quad \frac{\partial f_\tau}{\partial y} = 0, \; at \; y = L_y \tag{7b}$$

$$\lim_{r\to 0}\int_S \left[-V_r f_\tau - D_r \frac{\partial f_\tau}{\partial r}\right] dS = \frac{Q_O}{\theta B}\delta(\tau), \quad at \; pumping \; well \; (x_1, y_1) \tag{7c}$$

$$f_\tau = 0, at \; \tau = 0, \tag{7d}$$

where the V_r and D_r are the average velocity and dispersion coefficient along the normal direction to the pumping well, S is the boundary of the pumping well as $r \to 0$, and Q_o is the pumping rate. Note that the 2nd type boundary at the well in the FIT problem (Equation 4c) has become a third type boundary in this problem (Equation 7c). The travel time PDF for every possible location can be obtained by running only one simulation using Equations 6 and 7.

The BIT simulation result for the example is illustrated in Figure 3, which shows travel time PDF maps for three times: τ = 30 days, 40 days, and 60 days in the past. The model parameters are listed in Table 1. The capture zone moves in an upstream direction and spreads. The probability levels become more diffuse as you go further back in time, and uncertainty grows. The travel time PDF distribution is affected by the heterogeneity of the aquifer, and a high travel time probability tends to occur in the high conductivity area.

Let us compare the backward-in-time (BIT) solution to the forward-in-time (FIT) solution. Figures 4a and 4b present the BIT travel time PDFs, $f_\tau(\tau / X)$, vs. FIT arrival time PDFs for two potential source locations (80, 30) and (80, 20). Comparing 4a and 4b, the travel time PDF for a location in the higher conductivity area is higher than that for a location in the lower conductivity area. Two FIT simulations, one for each source, were needed to produce this figure, but only one BIT simulation. The small difference between results from the two methods is caused by minor errors in the numerical

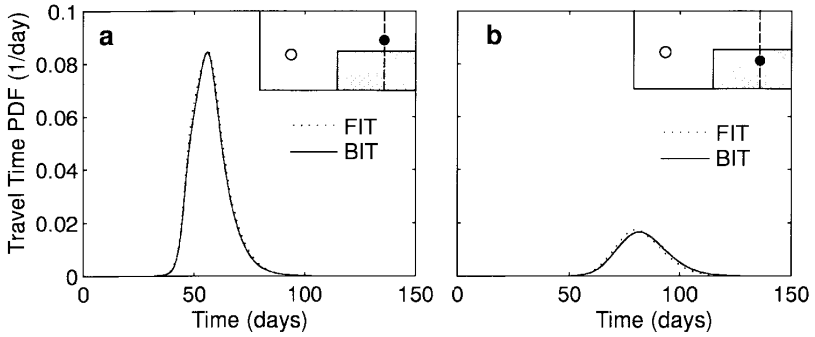

FIGURE 4. DIAGRAM OF THE TRAVEL TIME PDF, $f_\tau(\tau/X)$, VS. TRAVEL TIME FOR: a. THE SOURCE LOCATION AT (80, 30) AND b. THE SOURCE LOCATION AT (80, 20). THE DOTTED LINE SHOWS THE FORWARD-IN-TIME (FIT) SOLUTIONS, AND THE SOLID LINE SHOWS THE BACKWARD-IN-TIME (BIT) SOLUTION; TWO FIT SIMULATIONS ARE REQUIRED TO CONSTRUCT THIS FIGURE, BUT ONLY ONE BIT SIMULATION.

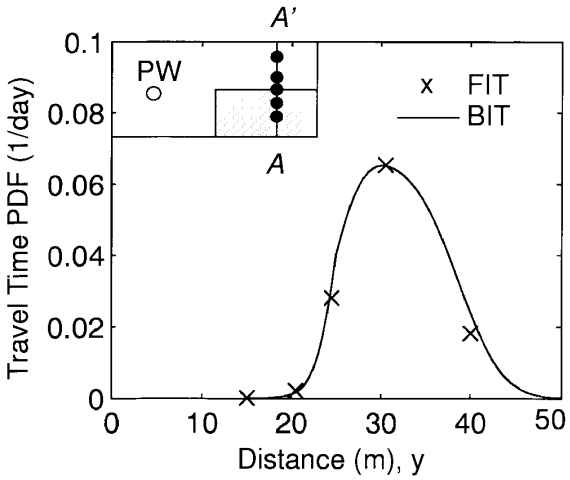

FIGURE 5. DIAGRAM OF THE TRAVEL TIME PDF VS. DISTANCE ALONG THE CROSS-SECTION *A-A'* AT x = 80 m. THE CROSSES REPRESENT THE TRAVEL TIME PDF FROM FIVE SEPARATE FORWARD-IN-TIME SOLUTIONS FOR SOURCE LOCATIONS: y = 15 m, 20 m, 25 m, 30 m, AND 40 m, RESPECTIVELY. THE SOLID LINE SHOWS ONE BACKWARD-IN-TIME SOLUTION ALONG THE SAME CROSS-SECTION.

simulation technique. The close comparison of results demonstrates that the travel time from any location in the aquifer, to the pumping well, can be estimated using either the BIT method or the FIT method, but the BIT approach is more efficient. Figure 5 amplifies these points. It shows the 60-day travel time PDF, from a single backward-in-time solution, for a cross-section through both locations (80, 20) and (80, 30). Also plotted are the arrival time PDFs from five separate FIT solutions.

The travel time cumulative distribution function (CDF), $F_\tau(\tau/X)$, describes the probability that a contaminant is captured by the pumping well in a period of time less than τ, from a given location, $X = (x, y)$ [1]. The travel time CDF, $F_\tau(\tau/X)$, can be obtained by integrating the travel time PDF, $f_\tau(\tau/X)$:

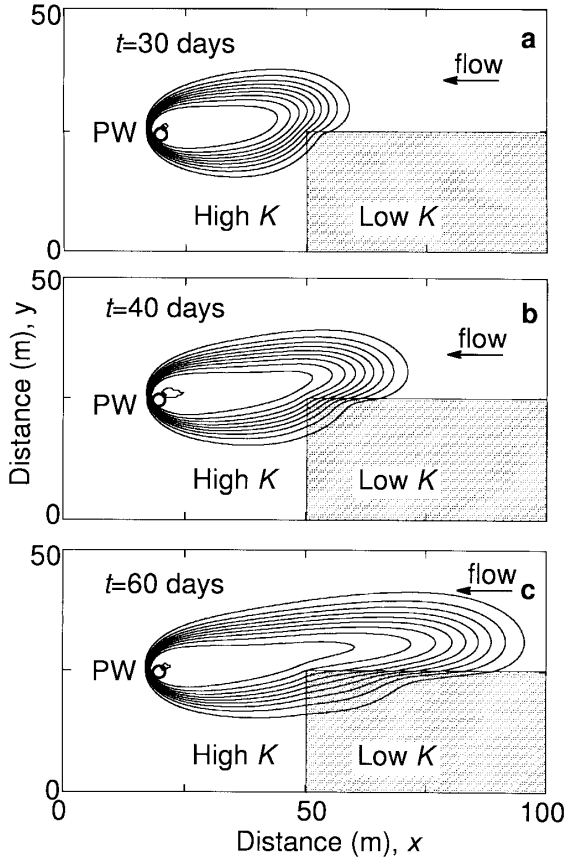

FIGURE 6. TWO-DIMENSIONAL TRAVEL TIME CDF FOR THE WELL. THE OUTERMOST CONTOUR LINE REPRESENTS PROBABILITY OF CAPTURE OF 0.1, AND THE CONTOUR INTERVAL VALUE IS 0.1. FIGURES a-c SHOW THE TRAVEL TIME CDFS FOR TRAVEL TIME LESS THAN 30 DAYS, 40 DAYS, AND 60 DAYS, RESPECTIVELY.

$$F_\tau(\tau|X) = \int_0^\tau f_\tau(\tau'|X)d\tau' . \tag{8}$$

In the new method, the travel time CDF can also be formulated from Equation 6 by replacing f_τ with F_τ, along with the boundary conditions:

$$\frac{\partial F_\tau}{\partial x} = 0,\ at\ x = 0;\quad F_\tau = 0,\ at\ x = L_x \tag{9a}$$

$$\frac{\partial F_\tau}{\partial y} = 0,\ at\ y = 0;\ \ \frac{\partial F_\tau}{\partial y} = 0,\ at\ y = L_y \tag{9b}$$

$$\lim_{r\to 0}\int_S \left[-V_r F_\tau - D_r \frac{\partial F_\tau}{\partial r}\right] dS = \frac{Q_O}{\theta B},\quad at\ \ pumping\ \ well\ \ (x_1, y_1) \tag{9c}$$

$$F_\tau = 0,\ at\ \ \tau = 0, \tag{9d}$$

where $F_\tau = F_\tau(\tau/X)$ is travel time CDF.

The travel time CDF can be computed by the following methods: 1) integration of the forward-in-time PDF for every possible source, 2) integration of the backward-in-time PDF, and 3) direct computation using the backward-in-time method. The solutions from all three methods are in very close agreement, differing only by a small amount attributable to numerical error. Figure 6 shows the travel time CDF, $F_\tau(\tau/x, y)$, for times: τ = 30 days, 40 days, and 60 days. The capture zone of the contaminant extends in an upstream direction for longer travel times, eventually spreading laterally to an asymptotic width. For the forward problem, the travel time CDF in this example had to be approximately reconstructed (not shown) by contouring the results of many simulations (100s) to approximate the continuous nature of $F_\tau(\tau/X)$; in practical multidimensional applications, with many potential source locations, it is unrealistic to obtain the CDF in this manner. Using the backward-in-time method, the travel time CDF is easily obtained by running one numerical simulation.

APPLICATION TO THE BORDEN TRACER TEST

We applied the backward-in-time method to a recent tracer experiment [2, 3] in order to demonstrate its use in applied problems and to validate it with field data. The experiment

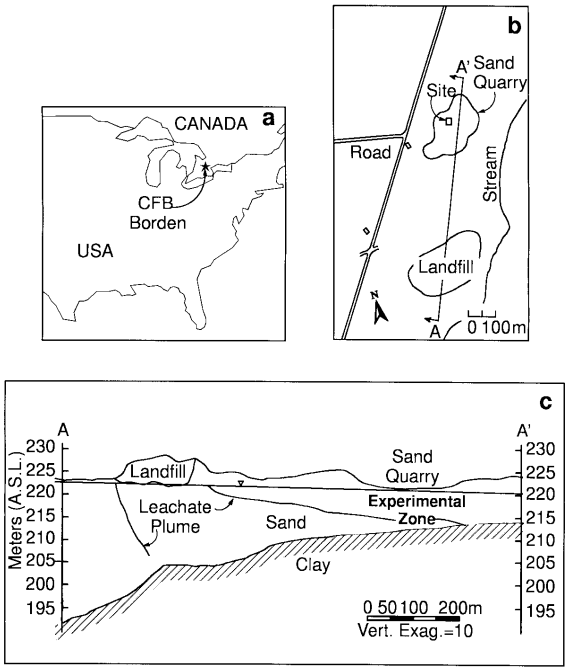

FIGURE 7. MAP OF THE BORDEN SITE TRACER TEST: a. MAP OF EASTERN USA AND SOUTHERN ONTARIO, CANADA, SHOWING GREAT LAKES REGION AND LOCATION OF CFB BORDEN; b. PLAN VIEW OF THE BORDEN SITE; c. SITE CROSS-SECTION (SCHEMATIC) *A-A'* SHOWING LANDFILL, EXPERIMENTAL ZONE, AND LOCAL GEOLOGIC FEATURES (AFTER LINDERFELT [3] AND MACKAY, *ET AL.* [14]).

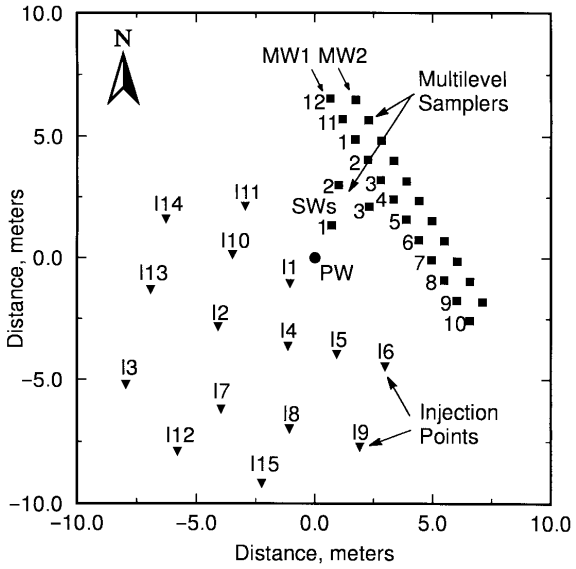

FIGURE 8. PLAN VIEW OF THE TRACER TEST SITE SHOWING LOCATION OF INJECTION POINTS, MULTILEVEL SAMPLING WELLS (MW AND SW) AND THE PUMPING WELL (PW) (AFTER LINDERFELT [3]).

was conducted by New Mexico Tech and the University of Waterloo, over the last half of 1992, at the Borden Canadian Forces Base in Ontario, Canada (Figure 7). The Borden aquifer is an eight meter thick, unconfined sand aquifer which is underlain by a thick, silty clay deposit [14]. Basic aquifer parameters, such as hydraulic conductivity, the dispersion coefficient, porosity, and the horizontal hydraulic gradient, have been studied in previous research (see summaries in [3] and [14]).

The experiment was designed to validate two-dimensional, vertically-integrated models of pumping well capture zones [2].

Tracers were injected upstream of the pumping well and monitored as they entered the well, or by-passed it, and moved through downstream multilevel samplers. The experiment site included one full penetrating pumping well, 15 injection points, and 26 multilevel samplers, as shown schematically in Figures 8 and 9. The time varying flow was from the southwest and south toward the northeast and north [15]. The pumping well produced from the aquifer at a constant rate, 2.16 m^3/day, for over four months [2]. Eight different tracers (7 fluorinated benzoic acids [FBAs] and bromide) were injected at 15 different locations upstream (i.e., southwest) of the pumping well. The injection mass and starting date for each tracer is shown in Table 2. The ground water samples collected in the pumping well were analyzed in the HPLC Lab at New Mexico Tech. The concentration breakthrough curves for four of the seven FBA tracers are shown in Figure 10.

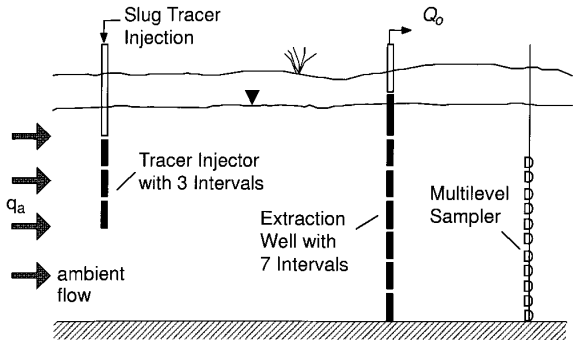

FIGURE 9. SCHEMATIC CROSS-SECTION OF THE BORDEN TRACER TEST WITH A FULLY PENETRATING PUMPING WELL (AFTER LINDERFELT [3]).

Ground water flow at the tracer test site

The numerical model used for this study covers an area of 30 x 30 m, centered on a point 5 m south of the pumping well, and oriented north and south. This geometry is illustrated in Figure 14, presented later. The axes origin is in the lower left hand corner. The pumping well is located at (15, 20), pumping at 2.16 m^3/day. Drawdown from this well is superposed on a natural regional gradient. Linderfelt and Wilson [2] suggest that the regional gradient is uniform in space but varying in time. Ground water heads in a large number of piezometers were measured weekly and used to construct the time-varying natural gradient magnitude, J_a, and direction angle, β [15]. The regional ambient flow rate, q_a, can be computed by the vertically integrated version of Darcy's law, $q_a = KBJ_a$ [L^2/T]. Superposing these two effects, the average velocity at the tracer test site is described by [2, 3]:

TABLE 2. TRACER INJECTION SITES, DATES, MASSES, AND NORMALIZED MASS RECOVERY FOR EACH OF THE INJECTION POINTS.

Injection			Tracer		Normalized mass recovery[b]		
Site	Date July	Day No.	FBA type[a]	Mass[c] (g)	66 days	117 days	124 days[c]
I1	1	0	o-TFMBA	30.2	1.00	1.00	1.00
I2	1	0	m-TFMBA	30.2	0.95	0.97	0.97
I3	6	5	3,4-DFBA	60.4	0.00	0.00	0.00
I4	1	0	PFBA	60.3	1.00	1.00	1.00
I5	1	0	2,3-DFBA	60.4	0.90	0.90	0.90
I6	3	2	2,6-DFBA	60.4	0.00	0.03	0.03
I7	6	5	3,5-DFBA	60.3	0.46	1.00	1.00
I8	3	2	2,3-DFBA	60.4	0.80	1.00	1.00
I9	3	2	PFBA	30.2	0.00	0.17	0.17
I10	1	0	3,4-DFBA	60.8	0.34	0.61	0.32
I11	3	2	3,5-DFBA	60.4	0.00	0.00	0.00
I12	6	5	PFBA	60.3	0.20	0.96	0.96
I13	3	2	o-TFMBA	60.4	0.00	0.00	0.00
I14	6	5	m-TFMBA	60.3	0.00	0.00	0.00
I15	6	5	2,6-DFBA	30.2	0.21	0.95	1.00

Notes: [a]DFBA = difluorobenzoic acid; TFMBA = trifluoromethylbenzoic acid; PFBA = pentafluorobenzoic acid;
[b]Normalized mass recovery; e.g., for t < 117 days = the ratio of mass recovered through 117 days to total mass injected.
[c]After Linderfelt [3].

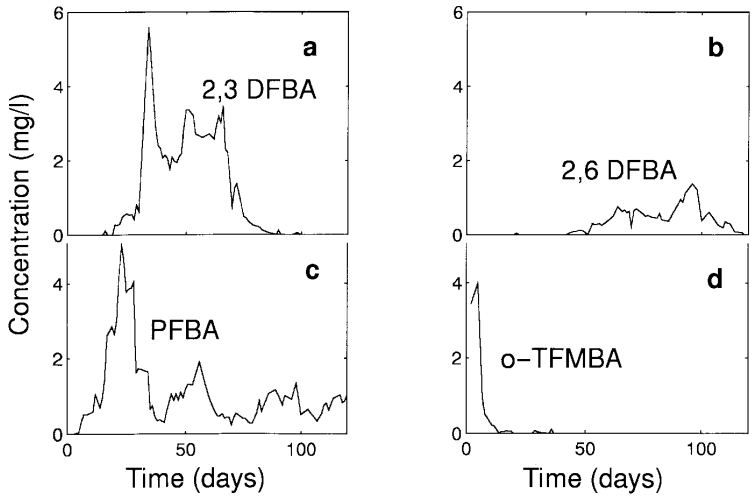

FIGURE 10. THE MEASURED VERTICALLY-INTEGRATED CONCENTRATION BREAKTHROUGH CURVES AT THE PUMPING WELL FOR 4 OF THE 8 TRACERS (AFTER LINDERFELT [3]).

$$V_x = \left[q_a \sin\beta - \frac{Q_O}{2\pi} \frac{x}{x^2 + y^2} \right] \frac{1}{\theta B}, \tag{10a}$$

$$V_y = \left[q_a \cos\beta - \frac{Q_O}{2\pi} \frac{y}{x^2 + y^2} \right] \frac{1}{\theta B}, \tag{10b}$$

where Q_o is the pumping rate [L^3/T], x is positive to the east, y is positive to the north, β is the compass angle, and B is the thickness of the aquifer [L].

Tracer transport model

Each tracer was injected into one or more injection points, then moved downstream and was possibly captured by the pumping well some time later. Not all of the injected tracer was captured [2, 3]. Two-dimensional forward-in-time tracer transport for this situation is described by Equation 3, with the boundary and initial conditions shown in Table 1. The FIT resident concentrations are simulated using the Laplace transform-in-time Galerkin finite element method [12]. The Laplace transform method requires a steady flow field. The flow field is provided by Equations 10a and 10b. The experiment was broken into three time periods, with steady flow roughly assumed in each period, as documented in Table 1. Other parameters utilized in these simulations are also listed in Table 1.

FIT pumping well arrival time distributions were simulated for injection sites I5 and I8, and are shown in Figures 11a and 11b, respectively, as the dotted lines. In the field test the same tracer, 2,3-DFBA, was injected at both points. The simulated joint arrival of this tracer from both injection locations is shown as the dotted line in Figure 11c. Compare to Figure 10a, keeping in mind that it is for concentrations, while Figure 11c is for arrival time probabilities. To compare the two, the concentrations must be normalized, as described below.

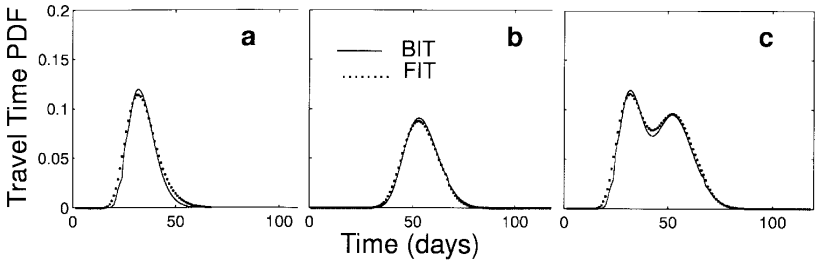

FIGURE 11. TRAVEL TIME PDFS FROM ONE BACKWARD-IN-TIME (BIT) SIMULATION COMPARED TO ARRIVAL TIME PDFS FROM TWO SEPARATE FORWARD-IN-TIME (FIT) SIMULATIONS OF INJECTIONS AT a. I5 AND b. I8. TRACER 2,3-DFBA WAS INJECTED AT BOTH OF THESE LOCATIONS, AS SIMULATED IN c BY COMBINING THE RESULTS OF a AND b. COMPARED TO ACTUAL TRACER ARRIVALS IN FIGURE 10a.

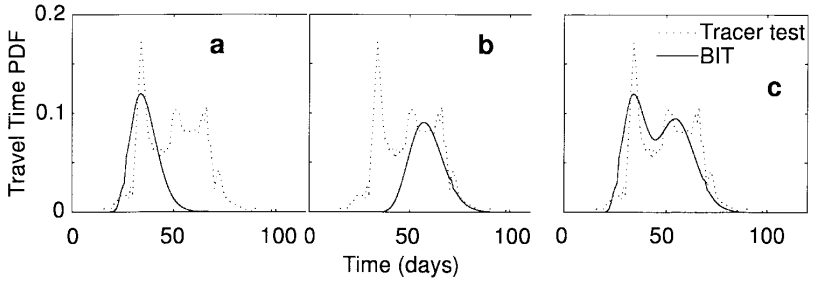

FIGURE 12. TRAVEL TIME PDFS FROM A SINGLE SIMULATION OF THE BACKWARD-IN-TIME (BIT) MODEL (SOLID LINES), COMPARED TO THE EMPIRICAL ARRIVAL TIME PDF (DOTTED LINES) CONSTRUCTED BY NORMALIZING THE BREAKTHROUGH CURVE BY THE INJECTED MASS OF TRACER 2,3-DFBA. SIMULATIONS FOR a. INJECTION POINT I5, b. INJECTION POINT I8, AND c. INJECTION POINTS I5 AND I8 TOGETHER. THE 2,3-DFBA EXPERIMENTAL BREAKTHROUGH CURVES HAVE BEEN NORMALIZED BY THE INJECTED MASS AT I5 AND I8.

Modeling arrival time of tracers using the backward-in-time method

The travel time backward-in-time model for this situation is expressed by adjoint Equation 6, with boundary and initial conditions given in Table 1. The solid lines in Figure 11 present the BIT travel time probabilities for 2,3-DFBA from injection sites I5 and I8, computed by one BIT simulation run, and compares it to the multiple FIT simulations of tracer transport. The two methods are in close agreement. The simulation is also compared to the tracer breakthrough data in Figure 12, which has been normalized by the total injected mass (Table 2) and replotted. Normalized breakthrough curves are estimates of the arrival time probability of the tracers [16, 17]. The same BIT travel time simulation run applies to all 15 injection sites. The simulated travel time distributions for three other tracers are plotted in Figure 13, along with their normalized breakthrough curves. Only previously published data are used [3]. No additional calibration or curve fitting has been done.

The tracer 2,3-DFBA was injected into I5 and I8, and the normalized concentration breakthrough curve observed from the pumping well is shown in Figure 12. Figure 12a shows that the travel time was about 32 days from I5 to the pumping well and that

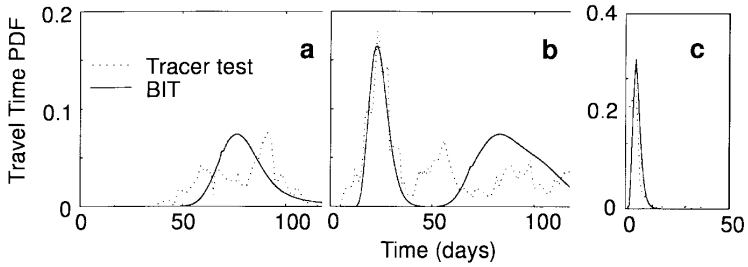

FIGURE 13. EMPIRICAL ARRIVAL TIME DISTRIBUTIONS (NORMALIZED BREAKTHROUGHS) AND SIMULATED BIT TRAVEL TIME PDFS FOR THE TRACERS a. 2,6-DFBA FROM I15, b. PFBA FROM I4, I9, AND I13, c. O-TFMBA FROM I1.

the simulation is very close to the first peak of the tracer 2,3-DFBA in shape. Figure 12b shows that the travel time is about 55 days from I8 to the pumping well and that the simulation can be fitted to the last two peaks of tracer 2,3-DFBA. For the complete interpretation of this tracer we need to consider the travel time probability for both injection points. Totaling their arrival time probabilities, Figure 12c presents the simulated travel time probability for both I5 and I8. It is close to the empirical arrival time curve of tracer 2,3-DFBA in shape. As a result, we can say that the first peak of tracer 2,3-DFBA represents the arrival of tracer from I5, while the last two peaks describe the arrival from I8.

The tracer 2,6-DFBA was injected into I6 and I15, and the normalized breakthrough curve is shown in Figure 13a. The simulations for I6 and I15 demonstrate that the tracer from I6 was not captured by the pumping well. Figure 13a only presents the simulated travel time probability for location I15. The estimated travel time from I15 to the pumping well is about 75 days. For the normalized concentration of 2,6-DFBA, the arrival time of the tracer ranged from 60 days to 95 days, with a most likely arrival time of 90 days. The comparison demonstrates that the simulations are reasonably close to the most likely arrival time.

The tracer p-TFMBA was injected into I4, I9, and I12. The normalized breakthrough curve and its BIT simulation are shown in Figure 13b. The empirical curve presents one high peak at about 20 days and three low peaks over a period of 50 days to 120 days. The simulated travel time probability for I4 agrees with the first peak of p-TFMBA, with a most likely travel time of about 20 days. The simulated travel time probability for I12 has a range of 66 days to 90 days, which is close to the third peak of p-TFMBA. The simulated (travel time) probability for I9 is much smaller, with a maximum close to the last peak of p-TFMBA. The total of the three travel time probabilities in Figure 13b can be favorably compared to the normalized breakthrough. As a result, the first high peak is the arrival of tracer from I4, and the third low peak is the arrival from I12. The last, small peak should include the arrival from I9. The second peak is probably also I12, which presumably split off and arrived earlier because of aquifer heterogeneity [3].

The tracer o-TFMBA was injected into I1 and I13, and the normalized breakthrough is shown in Figure 13c. The arrival time probability has one peak at about 5 days.

The simulation predicts that the only o-TFMBA tracer captured was from I1; the tracer from I13 flowed out through the multilevel sampler zone. The BIT simulated travel time from I1 to the pumping well is about 5 days, which agrees with the empirical arrival time of o-TFMBA.

Modeling the pumping well capture zone using the backward-in-time method

We simulated the tracer test capture zone by building travel time CDF maps using the backward-in-time model. These maps are compared to the measured time-dependent accumulation of normalized tracer mass in the pumping well. This is complicated by the fact that each tracer was injected in more than one well.

The cumulative mass of the tracer extracted from the pumping well can be computed using the concentration and pumping rate:

$$m_k = \sum_{i=1}^{k} C_i^f Q_O \Delta t_i , \qquad (11)$$

where m_k is the cumulative mass [M] for a time period $t = t_k = \Sigma\Delta t_i$, C_i^f is the flux concentration [M/L^3] observed in time t_i from the pumping well, and Q_o is the pumping rate [L^3/T]. The cumulative distribution or relative mass recovery for time $t = t_k$ can be computed by [16, 17]:

$$P(t' < t|x) = \frac{m_k}{M} , \qquad (12)$$

where $P(t' < t|x)$ is the cumulative distribution for time less than t, and M is the total mass injected into the aquifer. Linderfelt [3] computed the total cumulative mass produced by the well for eight types of tracer over the entire test period (to 124 days). We look at earlier times—66 and 117 days. Since each tracer was injected in more than one well, and since some of these multiple injections were produced in the pumping well (e.g., Figures 12c & 13b), it is necessary to separate the breakthrough curve mass for each tracer and assign it to individual injection points. The BIT arrival times could be used for this purpose. Instead we followed Linderfelt's [3] final separations, which were partly based on three-dimensional FIT simulations. Using these separations, the cumulative tracer production for each of the 15 injection sites is computed by Equations 11 and 12. The results are shown in the last three columns of Table 2; the last column is based on Figure 4-38 of Linderfelt [3].

For the backward-in-time model of the tracer test, the cumulative distribution of the travel time, $F_\tau(\tau|x)$, is described by adjoint Equation 6, with $F_\tau(\tau|x)$ as the state variable. The initial and boundary conditions are given by Equations 9a-d, with the exception that a zero gradient boundary is used at L_x. The BIT simulation of travel time CDF for the tracer experiment is presented in Figure 14, for a. travel times less than 66 days, and b. less than 117 days. The area surrounded by inner contour interval in these plots represents a 0.90 or greater probability of capture within the prescribed time period. The area outside of the outer contour interval has a less than 0.10 chance of capture. The simulated capture zone extends upstream as the travel time increases. Note also the slight shift in angular orientation of the capture zone, caused by the time varying flow field.

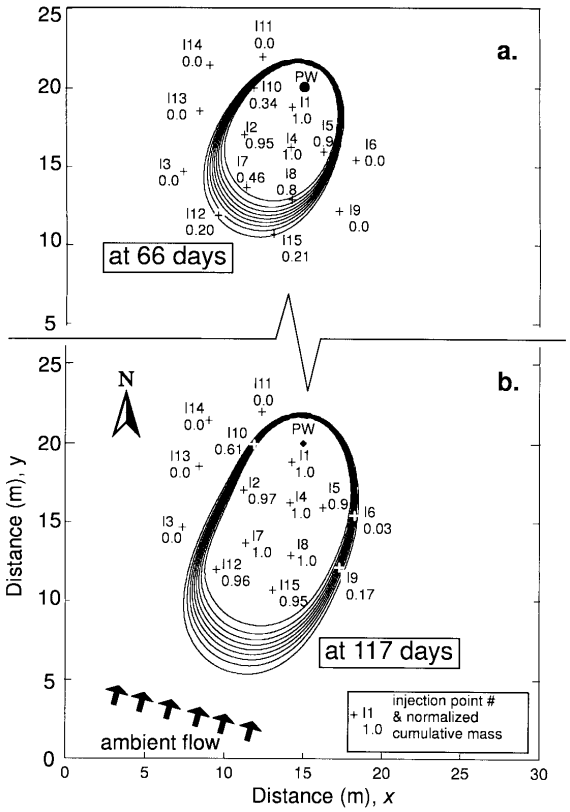

FIGURE 14. SIMULATION OF TRAVEL TIME CUMULATIVE DISTRIBUTION FUNCTION (CDF) FROM THE BACKWARD-IN-TIME METHOD, COMPARED TO NORMALIZED MASS ACCUMULATED IN THE PUMPING WELL FOR 7 TRACERS AT a. 66 DAYS AND b. 117 DAYS. THE CONTOUR INTERVAL IS 0.1, AND THE CONTOURS REPRESENT BIT SIMULATED PROBABILITIES OF CAPTURE, WITHIN THE PRESCRIBED TIME PERIOD, OF 90% ON THE INSIDE CONTOUR LINE, AND 10% ON THE OUTSIDE LINE.

At 66 days, Figure 14a indicates that injection points I1, I2, I4, and I5, with greater than 0.9 actual recovery, are appropriately located in the area where the BIT simulations of travel time probabilities predict recoveries greater than 0.9. Injection point I7 is also in the zone, but actually had only 0.46 recovery. Injection point I8, with an actual recovery of 0.8, is located near the 0.8 simulated contour line. The injection points I3, I6, I9, I11, I13, and I14, with no actual tracer recovery, are appropriately located where the simulations suggested zero recovery. Injection points I12 and I15 each had about 0.2 recovery and are located along the front of the predicted capture zone, about where they "should be." The only data inconsistent with the BIT simulations is from I7, with 0.46 actual recovery vs. a simulated recovery of greater than 0.9. In general, the simulations demonstrate a good match to the tracer test.

At 117 days, Figure 14b indicates that injection points I1, I2, I4, I5, I7, I8, I12, and I15 are located where the actual recoveries and simulated travel time capture probabilities are both larger than 0.9. Injection points I3, I11, I13, and I14 are located where actual and simulated recoveries are nil. Injection points I6, I9, and I10 are in the intermediate, dispersed zone, in both the BIT simulation and the data. The small differences between predicted and actual recoveries in this zone could be caused by the approximation of the transient flow field, aquifer heterogeneities, and other second order influences.

Experimentally-recovered tracer mass is assigned to 11 of the injection locations in Table 2—only 10 locations if you discount the small assignment to I6 (only 0.03). Tracer from 4, and perhaps 5, injection sites did not appear be recovered, apparently missing the pumping well. The BIT simulation predicted this response, suggesting that tracer from these same four wells would not make it to the well, and only a small amount would make it from the fifth. It appears that the backward-in-time method can be employed to delineate the capture zone of a pumping well.

SUMMARY AND CONCLUSIONS

This work demonstrates that, for a two-dimensional heterogeneous aquifer, contaminant travel time and location probability can be directly determined using the backward-in-time method, with results that are in close agreement with traditional forward-in-time methods and experimental data. We implemented and tested the backward-in-time method using a two-dimensional numerical model of flow and transport, accounting for advection and dispersion. The method was successfully applied to a variety of hypothetical problems and to a capture zone tracer test conducted at the Borden field site in Ontario, Canada. Some of the specific conclusions we have reached may be stated as follows:

- By proper selection of BIT initial and boundary conditions at the pumping well, maps for both travel time probability and location probability can be obtained for a two-dimensional model. The appropriate boundary condition for the travel time probability is a third type boundary condition at the pumping well, and it is described by a delta function for the PDF or a unit one for the CDF. The proper initial condition for the location PDF is a delta function distribution around the pumping well.
- In a two-dimensional aquifer, the travel time and location probability are directly simulated from the backward-in-time partial differential equations. The travel time probability can be compared to arrival time probabilities computed from multiple forward-in-time simulations.
- The backward-in-time method is employed to simulate normalized tracer breakthrough or arrival time probability for the Borden site capture zone tracer test. By running one backward-in-time simulation, we obtain the travel time probabilities for all injection sites. The simulations for most injection sites match the actual tracer arrival time probability very well, especially for the injection sites close to the pumping well.
- Using the backward-in-time model we delineate a travel time cumulative distribution map for the Border tracer test that is consistent with observed tracer recoveries.

ACKNOWLEDGMENT

The research on which this report is based was financed in part by the U.S. Department of Energy through the New Mexico Waste-management Education & Research Consortium (WERC). The field test was sponsored by the U.S. Environmental Protection Agency, grant number CR 818019-091-0, through the R.S. Kerr Laboratory.

REFERENCES

1. J.L. Wilson and J. Liu, Backward tracking to find the source of pollution, In: R. Bhada, *et al.* (Eds.), Waste-management: from Risk to Reduction, ECM Press, Albuquerque, New Mexico, 1995, pp. 181-199.

2. W.R. Linderfelt and J.L. Wilson, Field study of capture zones in a shallow sand aquifer, In: Th. Dracos and F. Stauffer (Eds.), Transport and Reactive Processes in Aquifers, Balkema, Rotterdam, 1994, pp. 289-294.

3. W.R. Linderfelt, Field Study of Capture Zones in a Shallow Sand Aquifer, Ph. D. Thesis, New Mexico Tech, Socorro, NM, 1994.

4. J. Liu and J.L. Wilson, Backward travel time and location probabilities for non-equilibrium sorption, Abstr., EOS, 75 (1994) 293.

5. J. Liu and J.L. Wilson, Modeling travel time and source location probabilities in two-dimensional heterogeneous aquifer, Proc. 5th Ann. WERC Tech. Devel. Conf., WERC, Las Cruces, New Mexico, 1995, pp. 59-67.

6. J.L. Wilson and S. Rao, The backward-in-time advection-dispersion problem, Abstr., EOS, 73 (1992) 134.

7. W.R. Linderfelt, J.L. Wilson, and S. Leppert, Capture zones for wellhead protection: Effect of time dependent pumping, saturated thickness, and uncertain parameters, Abstr., EOS, 70 (1989) 971.

8. G.J.M. Uffink, Application of Kolmogrorov's backward equation in random walk simulations of groundwater contaminant transport, In: H. Kobus and W. Kinzelbach (Eds.), Contaminant Transport in Groundwater, Balkema, Rotterdam, 1989, pp. 283-289.

9. J.L. Wilson and W.R. Linderfelt, Groundwater Quality In Pumping Wells Located Near Surface Water Bodies, Tech. Comp. Rpt. 261, New Mex. Water Resour. Res. Inst., Las Cruses, N.M., 1991, pp. 4.10-4.15.

10. A.C. Bagtzoglou, D.E. Dougherty, and A.F.B. Tompson, Application of particle methods to reliable identification of groundwater pollution sources, Water Resour. Man., 6 (1992) 15-23.

11. D. Chin and P.V.K. Chittaluru, Risk management in wellhead protection, J. Water Resour. Plan. and Man., 120 (1994) 293-315.

12. E. A. Sudicky and R.G. McLaren, The Laplace transform Galerkin technique for large-scale simulation of mass transport in discretely fracture porous formations, Water Resour. Res., 28 (1992) 499-513.

13. E.A. Sudicky and R.G. McLaren, User's Guide for Fractran: An Efficient Simulator for Two-dimensional, Saturated Groundwater Flow and Solute Transport in Porous or Discretely-fractured Porous Formations, Waterloo Centre for Groundwater Research, University of Waterloo, Ontario, Canada, 1991.

14. D.M. Mackay, D.L. Freyberg, P.V. Roberts, and J.A. Cherry, A natural gradient experiment on solute transport in a sand aquifer. 1. Approach and overview of plume movement, Water Resour. Res., 22 (1986) 2017-2029.

15. J.L. Wilson and W.R. Linderfelt, Field tracer experiment design problems at the Borden site, In: T. Bjornstad and G.A. Pope (Eds.), Proc. 2nd Tracer Workshop, Univ. of Texas at Austin, November 14-15, 1994, Rpt. IFE/KR/E-95/002, Inst. for Energy Technology, Kjeller, Norway, 1995, pp. 11-21.

16. W.A. Jury and F. Roth, Transfer Functions and Solute Movement through Soils, Birkhauser, Boston, 1990.

17. E.J. Henley and H. Kumamoto, Probabilistic Risk Assessment: Reliability Engineering, Design, and Analysis, IEEE Press, New York, 1992, pp. 245-264.